Successful Application of the Derived Crystal Packing (DCP) Model in Resolving the Crystal Structure of a Metastable Polymorph of (±) Modafinil[†]

Morgan Pauchet,[#] Claire Gervais,[‡] Laurent Courvoisier,[§] and Gérard Coquerel*,[#]

Unité de Croissance Cristalline, de Chromatographie et de Modélisation Moléculaire (UC3M2) Sciences et Méthodes Séparatives (SMS), UPRES EA 3233, IRCOF, Université de ROUEN, 76821 Mont-Saint-Aignan Cedex, France, Department of Chemistry & Biochemistry, University of Berne Freiestrasse 3, CH-3012 Berne, Switzerland, and Cephalon France Z.I. Mitry-Compans, 77 292 Mitry Mory Cedex, France

ABSTRACT: Polymorphic forms I and III of (±) modafinil have been studied. In contrast to the structure of form I which could be solved by using conventional single crystal X-ray diffraction, the crystal structure of form III could not be elucidated due to the shape and the size of the single crystals resulting from the high supersaturation under which this phase is obtained. To bypass the problem, the derived crystal packing (DCP) model has been successfully applied by recombining the slice (002)A extracted from form I. The calculated XRPD pattern of form III fits well with the experimental data. The extensive similarities between the two crystal structures are carefully detailed.

Introduction

Polymorphism, defined as the ability for a molecule (or a set of molecules) to adopt several packing arrangements, became in the past decades a field of research on its own. Among other advantages of studying polymorphic systems, one can cite the study of the influence of molecular packing on solid-state properties, a better understanding of nucleation and crystal growth mechanisms, and control of bioavailability and processes in pharmaceutical industry. Because polymorphism can have a high impact on the solid-state properties, it is important to thoroughly characterize every polymorphic form that may be encountered during the development of a compound. However, it can be difficult to obtain accurate results concerning one particular polymorphic form. Many problems can occur, such as metastable or unstable phases with a high transformation rate, concomitant polymorphism[1] (difficulties in obtaining a high structural purity), poor crystallinity, etc.[2] When experimental analyses fail, structure prediction tools can be used to propose possible polymorphic forms. Prediction results can then be compared with available experimental data to find a match that could ascertain the structure of the compound.

Structure predictions are usually divided into two categories: ab initio predictions and crystal engineering. Ab initio predictions[3,4] start from a "zero-dimensional" structure, i.e., the molecule or a set of molecules only. A number of candidate structures is obtained, either by successively adding symmetry operators to regenerate the three dimensions and optimizing the potential energy at each step, or by packing the molecules in unit-cells of several dimensions and space groups, and optimizing and selecting low-energy structures. The program PROMET by Gavezzotti,[5] for example, has been developed for this purpose as a method inspired by Kitaigorodskii's Aufbau Principle[6] used by Perlstein.[4] The large number of predicted structures can however be a drawback. Whereas the experimental form is likely to be found among them, the energetic differences between the structures are often small, so that an identification of the potentially appearing forms becomes problematic.[3,7] Another approach to predict crystal structure is to perform a crystal engineering study. Structures of compounds possessing similar chemical entities or intermolecular interactions (hydrogen bonds, π–π stacking, halogen–halogen interactions...) are analyzed and information is exploited to design supramolecular synthons which are expected to generate structures with given properties.[8] Contrary to ab initio predictions, which focus on the research of crystal structures of a given molecule, the design of architectures with desired properties (the molecule itself having, in some ways, a minor role) is the main goal of crystal engineering. Therefore, such a method cannot be directly used for structure prediction, and has to be combined with other procedures to come into practice.[9]

The derived crystal packing model (hereafter, DCP model), which allows one to predict new crystal packings starting from a known structure, shares some similarities with the aforementioned approaches. It can be used as an alternative way to predict the structure of possible polymorphic forms,[10] particularly when additional information about common structural features between the known and the unknown varieties are available or at least suspected. The example treated here is the marketed drug (±) modafinil, 2-(diphenylmethyl) sulfinyl)-*N*-acetamide. Up to now, six polymorphic forms and several solvates of (±) modafinil have been observed.[11,12] Among these, we will focus here on two asolvate polymorphs, i.e., form I which is the stable and commercially available form and the metastable form III.
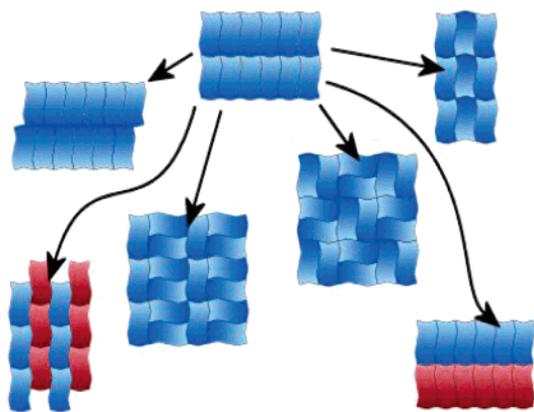
Figure 1. Two-dimensional examples of several daughter phases built from the same mother phase (in red, PF regenerated by a mirror or a glide plane).

Form III crystallizes concomitantly with form I and adopts generally a St. Andrew cross shape. Resolution attempts either by single-crystal X-ray diffraction or powder diffraction were not crown with success. However, analyses of the XRPD patterns revealed that form III seems to share structural features with form I, so that application of the DCP model to resolve the crystal structure of form III is a method of choice.

After a short explanation of the "philosophy" of the DCP model (thoroughly described in a previous paper[10]), experimental procedures to obtain form I and form III of (±) modafinil are presented. Then, in sequence, the paper deals with (i) the examination of the XRPD patterns combined with a structural analysis of form I so that putative common structural features belonging to forms I and III could be pointed out; (ii) the extraction of periodic fragments from form I and the regeneration of possible 3D crystal packings of form III; and (iii) an extended comparison of the structures of the two forms. Some possible consequences of their structural similarities are proposed.

Description of the DCP Model

The application of the DCP model relies on the existence of common arrangements of the molecules in two polymorphic forms (couples of enantiomers and racemic compounds might also be derived from one another by this type of structural relationship). If signs of similarities are suspected between two forms (such as the propensity for a family of compounds to conserve the same arrangement inside a layer, or common peaks at low θ on X-ray powder diffraction patterns revealing identical reticular distances), the DCP model is worth testing. In its present version, the DCP procedure can be divided into two consecutive steps illustrated in Figure 1:

(1) *Extraction of periodic fragments* (hereafter PF) from a mother phase. A PF contains one or several molecules of the asymmetric unit (if $Z' \neq 1$) periodically regenerated (by means of translations along the *a*, *b* or *c* axis, or any other crystallographic symmetries) along one or two directions, forming a ribbon or a slice, respectively.

(2) *Generation of three-dimensional structures* (called daughter phases) by addition of *symmetry operators*.

One or two symmetry operators are added respectively to the slice or to the ribbon. Depending on the location and the nature of the operators added, several final structures can be obtained starting from the same periodic fragment.

The number of possible PF that can be extracted from a single-crystal structure being quite large (it increases with Z and Z'), it is in practice necessary to limit the number of extracted fragments. Although it is in principle possible, the DCP model is not intended to handle hundreds of potential structures contrary to ab initio predictions. The PFs are chosen by considering molecular interactions (e.g., ionic bonds, hydrogen bonds, $\pi-\pi$ interactions), which are mainly responsible for the stability of the mother structure. For instance, two-dimensional hydrogen-bond networks form slices of molecules with low (negative) slice energies. Choosing such slices as PFs ensures already to the daughter phases a relative stability. Provided that the inter-PF energy is sufficiently low, one may expect that these daughter phases will possess lattice energies close to that of the mother phase. Therefore, PFs containing interactions such as ionic bonds, hydrogen bonds or $\pi-\pi$ interactions should be preferred in this order. Their identification can be done by performing a regular periodic bond chain (PBC) analysis.[13]

Once the PFs are selected, symmetry operations are performed on the them to regenerate 3D daughter phases. Crystallographic considerations about the locations of the symmetry operators and the consequences on the final space group and number of molecules in the asymmetric unit (Z') are detailed in a previous work.[10] To summarize, placing a symmetry operator on a general position can break symmetries contained in the PF (becoming then local symmetries) and give a daughter phase with a higher number of independent molecules. Whereas the number of daughter phases that can be derived from a single PF can be easily unmanageable, the choice of the final space group is however usually limited to the most populated space groups among organic crystals, i.e., $P1^*$, $P\bar{1}$, $P2_1^*$, $P2_1/c$, $C2/c$, $P2_12_12_1^*$, $C2^*$ $Pbca$, $Pnma$, $Pca2_1$, $Pna2_1$, $P2_12_12^{*3,14}$ (starred space groups correspond to restriction in symmetry for pure chiral molecule). Once the operators are positioned, the periodicity of the daughter phase is rebuilt by using Cerius^2 modeling software.[15]

Computational Scheme Applied during the Construction. As the PF is similar in both mother and daughter phases, their energy difference arises from the interface between the PFs. During the construction of the daughter phase, such interface energy is minimized by avoiding sterical bumps and keeping a density similar to that of the mother phase (Gavezzotti et al. showed in a study on the polymorphism of 204 compounds that 93% among them had a density difference lower than 5%[14]). To achieve this minimization, a docking procedure using SYBYL software[16] is performed. It consists of computing the inter-PF energy surface, and locating local minima corresponding to the lowest attachment energies between two PFs. It is worth noting that several minima may be obtained at different locations from the same PF and symmetry operators, leading thus to several potential daughter phases.
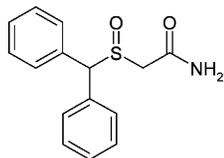
Figure 2. Developed formula of modafinil ((2-(diphenyl-methyl) sulfinyl)-*N*-acetamide).

The total intra-PF interaction energy is computed by summing all atomic−atomic interaction energies between the PFs. These energies are calculated by summing van der Waals repulsive and attractive interactions from the Tripos force field[16] as well as electrostatic interactions.[17] Gasteiger charges are computed for every atom of the PF. A grid point approximation similar to those found in the program GRID is used[18] to perform the calculations (potentials are computed at "grid points" and the contribution for an atom is assumed to be the same as the nearest grid point).

Finally, to compare the energies of the mother phase and the daughter phase, both structures are minimized by using the "minimizer" module of Cerius^2. Dreiding force field 2.21[19] is used. MOPAC charges[20] using the AM1 method[21] are assigned to the atoms. Ewald summations are done on both Coulombic and van der Waals interactions. Minimization is performed by using the "smart minimizer" with a standard convergence (maximum of 500 iterations). Neither this force field nor another force field was found to accurately optimize the structure of modafinil form I (without restraint a significant deviation of the cell parameters is observed). However, the bias introduced by the optimization procedure is assumed to exist also in the daughter phases. This hypothesis is reinforced by the fact that both structures share extensive structural relationships. To ensure a sufficient stability of the derived phase, the energy should not exceed that of the mother phase by more than a few kJ mol^{-1}.

Application to (±) Modafinil

Presentation of the Two Polymorphic Forms. Form I of (±) modafinil (Figure 2) can be obtained together with form III, by using a precipitation procedure followed by a fast filtration in various solvents, such as methanol, 2-methoxyethanol, acetone, ethanol, or a mixture of methanol and water (used as antisolvent). Concomitant polymorphism[1] can be avoided and single crystals of pure form I obtained by slowly evaporating a solution of methanol saturated in (±) modafinil at 20 °C (280 mg of (±) modafinil in 10 g of methanol) followed by cooling to 4 °C. A structural study
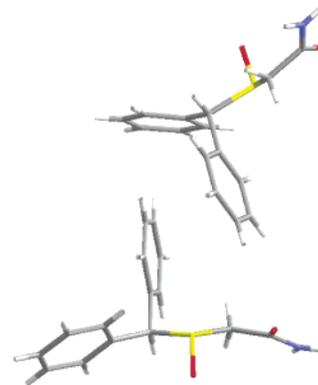

Figure 3. Asymmetric unit of (±) modafinil form I.
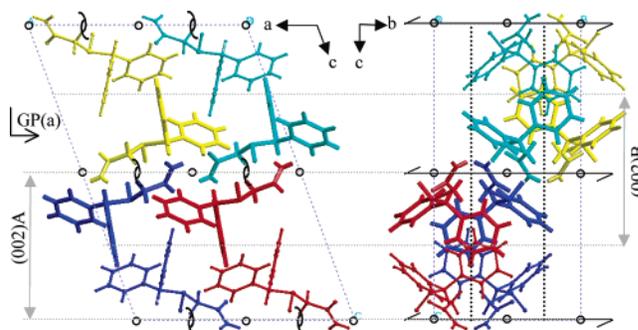

Figure 4. Projection along the *b* axis (left) and *a* axis (right) of the unit-cell of (±) modafinil form I. The asymmetric unit is in blue (the first molecule of the asymmetric unit is represented in bold with respect to the second one). Colors are used to depict the link with the symmetry operators: glide plane (a) in red, 2-fold screw axis in yellow, and inversion center in turquoise blue.

carried out by single-crystal X-ray diffraction on SMART APEX Bruker diffractometer revealed that form I belongs to the space group $P2_1/a$, with the following crystallographic parameters: $a = 14.502$ Å, $b = 9.688$ Å, $c = 20.844$ Å, $\beta = 110.17°$ (calculated density $\rho = 1.321$, see Table 1). XRPD patterns obtained from ground single crystals could be fully indexed by these crystallographic parameters.

As displayed in Figure 3, there are two molecules in the asymmetric unit. As often encountered in such a case, conformations of both independent molecules shown in Table 2 are very similar (80% of the case with $Z' = 2$).[22]

The molecular arrangement shown in Figures 4 and 5 can be described as a stacking of hydrogen-bonded (002)A layers or by a stacking of (002)B phenyl layers.[23] Slice (002)A contains both molecules of the asymmetric unit linked by $\pi-\pi$ interactions. A T-shaped arrange-

Table 1. Crystal Data, Data Collection, and Refinement of (±) Modafinil Form I

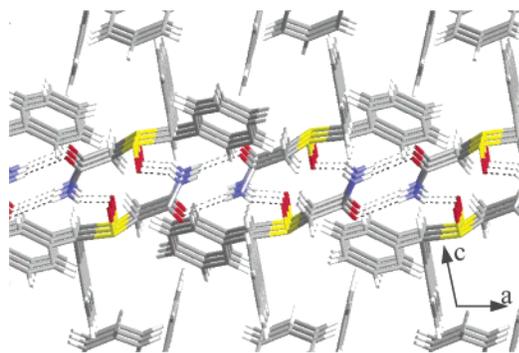|			
$C_{15}H_{15}NO_2S$	$M_r = 273.34$	Bruker SMART APEX diffractometer	
monoclinic, $P2_1/a$	$Z = 8$		
$a = 14.5022(1)$ Å	$\theta = 2.07-26.33°$	5621 independent reflections	$R_{int} = 0.018$
$b = 9.6875(8)$ Å	$\mu = 0.230$	5018 reflections with $I > 2\sigma(I)$	$\theta_{max} = 26.33°$
$c = 20.8445(2)$ Å	$T = 296$ K		$h = -18 \rightarrow 18$
$\beta = 110.1700(1)°$	prismatic, colorless	$T_{min} = 0.815$, $T_{max} = 1.000$	$k = -11 \rightarrow 12$
$V = 2748.85(4)$ Å^3	$0.60 \times 0.40 \times 0.40$	21392 reflections	$l = -26 \rightarrow 26$
refinement on F^2			
$R[F^2 > 2\sigma(F^2)] = 0.0359$		$W = 1/[\sigma^2(F_o^2) + (0.0603P)^2 + 0.6088P]$ where $P = (F_o^2 + 2F_c^2)/3$	
$wR(F^2) = 0.0997$		$(\Delta/\sigma)_{max} < 0.001$	
$S = 1.029$		427 parameters	
5621 reflections			

Figure 5. Detail of the structure of form I showing the hydrogen-bond network in dotted lines, spreading along *a* and *b*. Three unit-cells are projected in perspective along *b*.

ment between the phenyl groups is observed. The angle between the planes formed by two adjacent phenyl groups is alternatively 83.4° and 85.9° with distances between their geometric centers of 5.12 and 4.78 Å. The (002)A layers can be periodically repeated through space by using the inversion center or the 2-fold screw axis, leading to the 3D crystal packing of form I. Slice (002)B is composed of a two-dimensional hydrogen-bond network defined by $C=O\cdots H-N$ and $S=O\cdots H-N$ interactions. This network runs along the *a* and *b* axes and contains only one of the two molecules of the asymmetric unit, so that the whole structure cannot be rebuilt from (002)B by addition of symmetry operators. Slices (002)A and (002)B are shifted along the *c* axis by half the thickness of their common interplanar distance (i.e. d_{004}).

Whereas single crystals of form I were readily obtained, difficulties arise when trying to isolate form III. Various experiments were designed in acetonitrile, acetone, or a mixture of water and methanol. However, concomitant polymorphism[1] was observed, i.e., the obtained crystals were reproducibly of both forms I and III. By varying different parameters such as the introduction rate of (±) modafinil methanolic solution in cold water, the stirring rate, and the final relative amount of water and methanol, the following procedure leading to almost pure form III could be set up: in a double-walled thermostated reactor (0.5 °C), a solution of (±) modafinil (97 g) in methanol (759 mL) is poured into 600 mL of water (antisolvent). The stirring rate is set to 300 rpm during the experiment. Crystals are im-

mediately removed by filtration. The XRPD pattern confirms that "pure" form III is obtained (i.e., according to the detection limit). It is worth noting that small changes in the time spent before or during the filtration may induce the presence of the polymorphic form I. The poor quality of the XRPD patterns could not allow any determination of the structure nor even any automatic indexation of the peaks.

Particles obtained were observed by scanning electronic microscopy (SEM). They show twinned dendritic bodies in the shape of a St. Andrew cross (Figure 6) revealing a nucleation and a crystal growth far from thermodynamic equilibrium (crystals grew rapidly in the shape of needles, without well-defined faces). The presence of dendrites testifies of the crystal growth conditions that are far from equilibrium.

Thus, experimental conditions used for nucleation and crystal growth did not allow one to obtain single crystals of the size and quality required for the resolution of the structure by single-crystal X-ray diffraction.

Comparison between XRPD Patterns. The comparison between XRPD patterns of form I and form III displayed in Figure 7 reveals that the two first XRPD peaks (002 and 011 indexed with Miller indices of form I) overlap in both forms. From these two couples of overlapping peaks it can be surmised that form I and form III have at least two *d* spacings (equal to d_{002} and d_{011}), or even some unit-cell parameters in common. It is thus likely that there is a common slice in both forms that is appropriate for the application of the DCP model. Application on this slice of convenient symmetry operators could generate either the structure of form I or that of form III. This assumption is also consistent with the concomitant polymorphism observed between the two forms. Indeed, heteronucleation of one form on the other one can take place because of structural similarities leading to very close lattice energies.[24,25]

Detailed Description of Steps 1 and 2 on (±) Modafinil. Several attempts were made to find the common slice, extract it from form I, and generate suitable daughter phases with a correct lattice energy. Two PFs defined by (002)A and (002)B are able to generate plausible packings (i.e., with a density close to that of form I and without steric bumps between slices). (002)A is composed of the two independent molecules of the asymmetric unit, and contains as symmetries the glide plane *a*, and the translations along *a* and *b* (see Figure 8). (002)B is composed of one
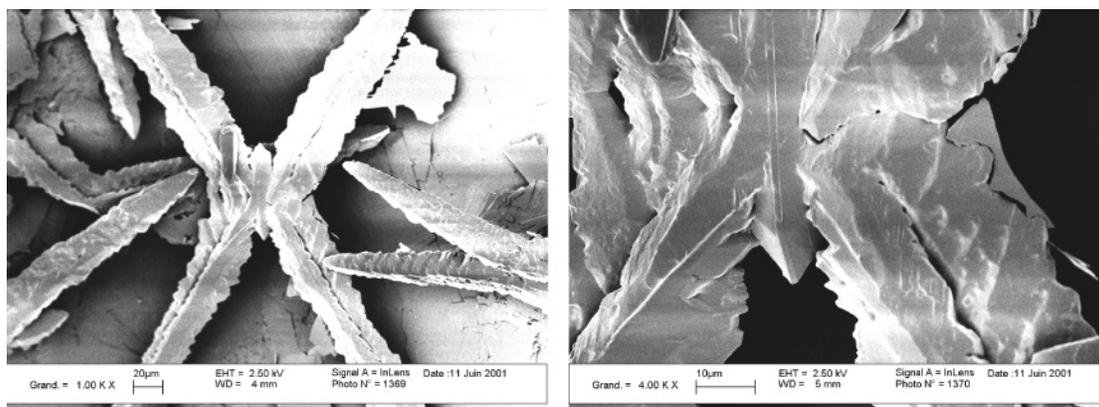

Figure 6. SEM micrographs of form III showing twinned dendritic bodies in the shape of St. Andrew cross.
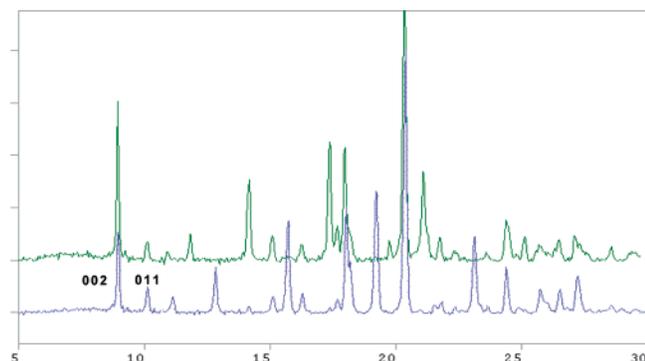
Figure 7. XRPD patterns (diffraction angles 2θ vs intensity with arbitrary scale) of form I (bottom) and III (up) of modafinil. (002) are the Miller indices of the common slice used to regenerate form III from form I.

molecule of the asymmetric unit and possesses the glide plane a, the 2-fold screw axis, the inversion center, and translations a and b as internal symmetries (see Figure 9).

Hereafter, we will focus on slice (002)A for which the construction of the daughter phase is more straightforward. Construction of a daughter phase using slice (002)B involves the creation of pseudo-symmetry and will therefore be discussed later.

The generation of a probable daughter phase (i.e., with a low lattice energy) is achieved by adding a 2-fold screw axis orthogonal to (002)A. The position of the added symmetry operator has been determined by taking into account the presence of the glide plane at $b = 1/4$ and $b = 3/4$. Only locations at $b = 0$ or $b = 1/4$ respect this glide plane symmetry, leading respectively to $Pna2_1$ and $Pca2_1$ with $Z' = 2$. Due to the topology of the PF, the latter position creates too much steric hindrance for a competitive density, so that only location at $b = 0$ gives a low inter-PF energy (Figure 10). The position of the 2-fold screw axis according to the axis a and its associated translation (which will be half of the

c parameter of the daughter phase) are set by the docking procedure presented in the first part of the paper (Figure 11).

A minimum "valley" with the highest density has been found by generating a daughter phase $Pna2_1$ with $c = 20.74$ Å. A hydrogen-bond network almost identical to that of form I has been created during this procedure. Obviously, the same result can be obtained by starting from the same slice (002)A and adding a glide plane n (orthogonal to the PF and to the glide plane a). It will implicitly generate the same 2-fold screw axis, and thus the same daughter phase.

From the nonoptimized daughter phase, a first simulated XRPD pattern very similar to the experimental one is computed. However, peaks related to the parameter c (i.e., hkl with $l \neq 0$) do not exactly match between both patterns. As previously mentioned, a minimization is not appropriate to retrieve the good crystallographic parameters, since it will converge toward a structure too different for both the mother and the daughter phase. To fit both XRPD patterns and to avoid the bias introduced by the minimization, the c parameter of the daughter phase is "manually" adjusted ±0.01 Å (i.e., the c value which is related to the distance between the PFs is slightly modified) and simulated XRPD patterns computed until the best match is obtained. At this stage, a Rietveld refinement would have been beneficial to the quality of the simulated structure. Nevertheless, the unavoidable poor quality of the XRPD pattern of form III left this Rietveld refinement out of consideration. The following parameters are obtained: $a = 14.50$ Å, $b = 9.68$ Å, $c = 19.76$ Å. As shown in Figure 12, the first two peaks of the XRPD patterns correspond to the (002) and (011) d_{hkl} spacings with 2θ values of 8.949° and 10.169°, respectively (experimental values 8.96° and 10.12°).

So as to ascertain the stability of the structure compared to form I, the daughter phase (DP) and the mother phase (MP) are optimized while keeping the
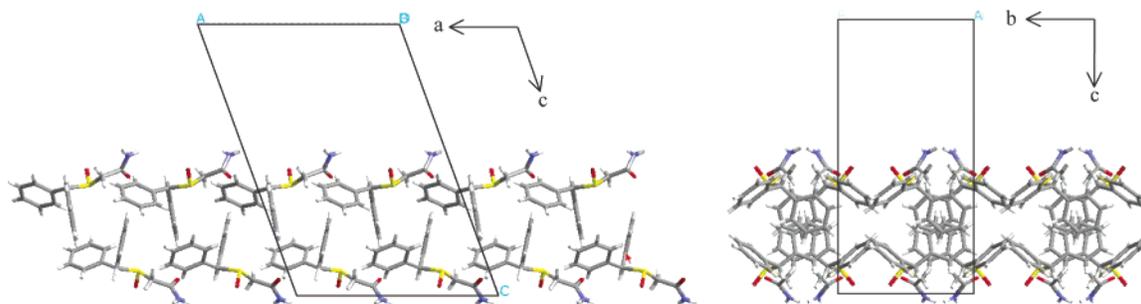

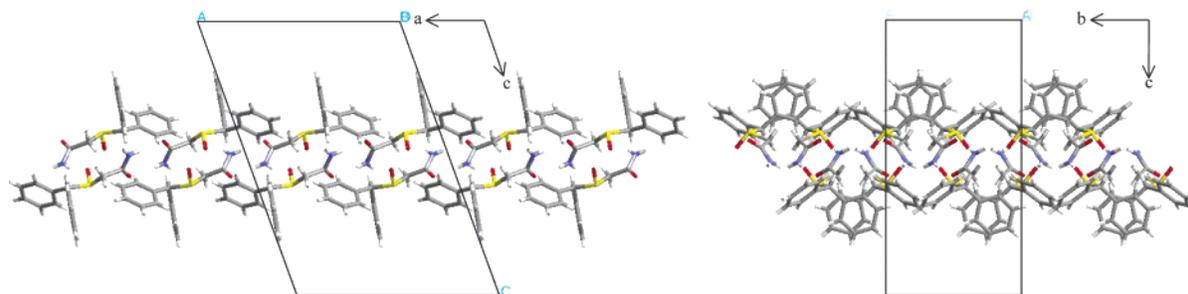**Figure 8.** PF (002)A: translations along a and b and glide plane (a).

Figure 9. PF (002)B: translation along a and b, glide plane (a), 2-fold screw axis and inversion center.
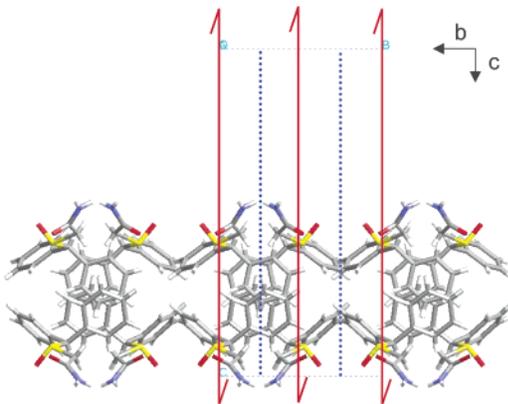
Figure 10. The 2-fold screw axis (red) must be added at $b = 0$ to give a consistent set of symmetries with the glide plane (blue) and to avoid steric hindrance.
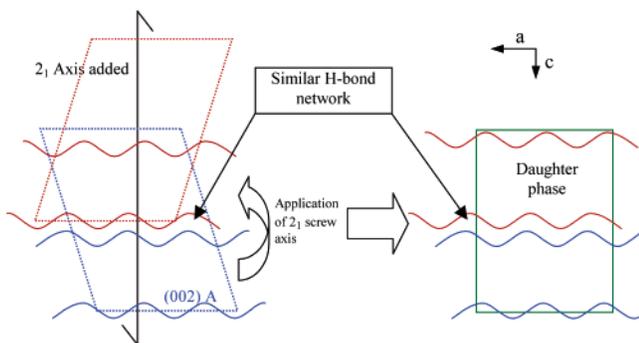

Figure 11. Addition of a 2_1 screw axis to the extracted (002)A slice and generation of the orthorhombic form.

cell parameters unchanged. The energy of the mother phase is taken as a reference and $\Delta E = E_{DP} - E_{MP}$ is presented in Table 3. The energy differences are among the margin usually observed between two polymorphic forms.

Owing to the match between the XRPD patterns (Figure 12) and the small lattice energy differences computed (Table 3), it can be concluded that the form III of (±) modafinil is likely to be described by the

Table 2. Torsion Angles in the Two Molecules of the Asymmetric Unit of (±) Modafinil Form I

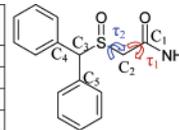|	Torsion Angle	Molecule 1 R enantiomer	Molecule 2 R enantiomer
τ_1	$- N - C_1 - C_2 - S -$	154.572°	146.785°
τ_2	$- C_1 - C_2 - S - C_3 -$	-172.657°	-170.123°
τ_3	$- C_2 - S - C_3 - C_4 -$	-63.576°	-59.339°
τ_4	$- C_2 - S - C_3 - C_5 -$	169.710°	174.521°

Table 3. Energy Differences in kJ mol^{-1} between the Mother Phase (MP: taken as reference) and the Generated Daughter Phase DP before and after Adjustment^a

	DP	DP adjusted	MP
a (Å)	14.50	14.50	14.502
b (Å)	9.69	9.69	9.688
c (Å)	20.74	19.76	20.844
β (°)			110.17
ΔE (kJ mol^{-1}) (molecules as rigid bodies)	+44.9	+13.3	0
ΔE (kJ mol^{-1}) (free molecules)	+6.4	+7.0	0
density	1.246	1.308	1.321
Δd (%)	5.68	0.98	0

^{a} The density is computed at 20° and Δd represents the density difference in % between the mother phase and the daughter phase.

generated daughter phase, and belongs to the space group $Pna2_1$ with $Z' = 2$ and $a = 14.50$ Å, $b = 9.68$ Å, $c = 19.76$ Å. (Fractional coordinates, intramolecular distances, angles, torsion angles, and hydrogen-bond distances for the daughter phase, the mother phase, and the minimized mother phase are collected in Supporting Information).

Extended Comparisons between Lattices of Form I and Form III. In Figure 13, nonprime and prime are used to discriminate the two molecules of the asymmetric unit. A comparison of the position of the molecules reveals that R3$'_{ortho}$ and S4$'_{ortho}$ are located in the same place as R3$_{mono}$ and S4$_{mono}$ but exhibit a different conformation. Therefore, the inversion center and 2-fold screw axis linking R1 with R3 and S2 with S4 in the monoclinic form become pseudo-symmetries in the orthorhombic form. Such a result must draw attention to the fact that the other (002) PF, named (002)B, can be used to generate the same daughter phase, provided
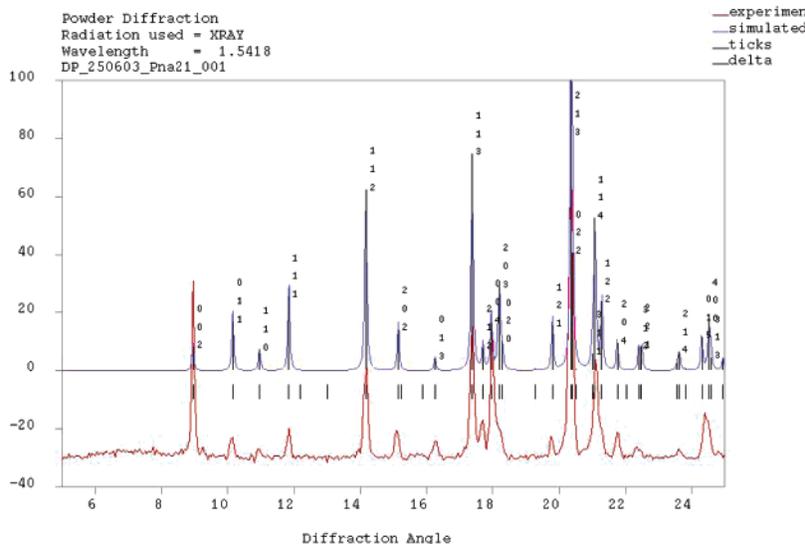

Figure 12. Experimental XRPD pattern (diffraction angles 2θ vs intensity with arbitrary scale) of form III and simulated XRPD pattern of the daughter phase.
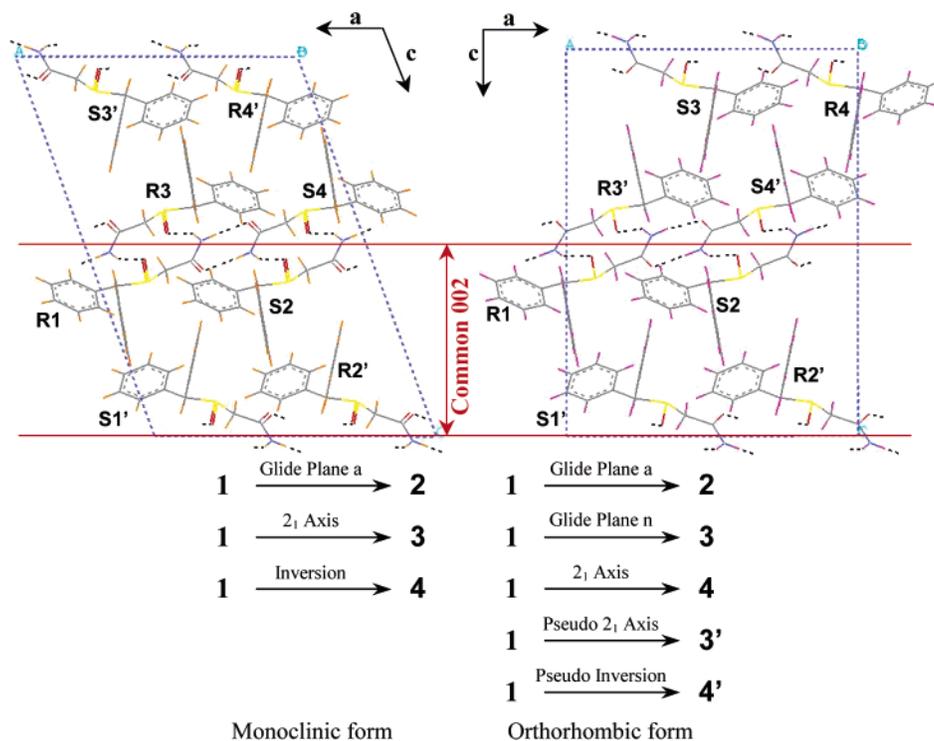
Figure 13. Relation between molecules in (±) modafinil form I (monoclinic) and form III (orthorhombic). Equivalent molecules of the unit-cell are numbered "1, 2, ..." according to the symmetry operator. The second molecule of the asymmetric unit is labeled with a "prime".
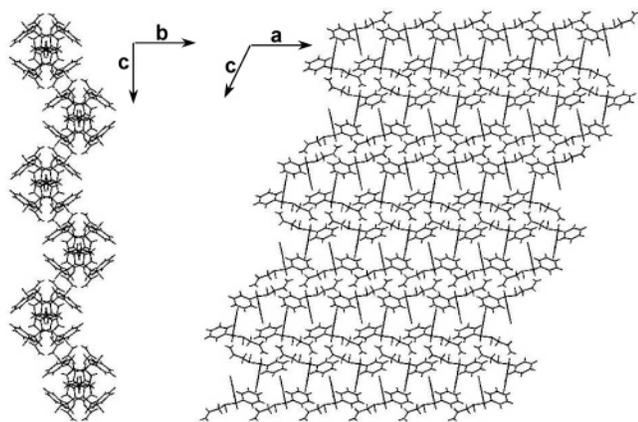

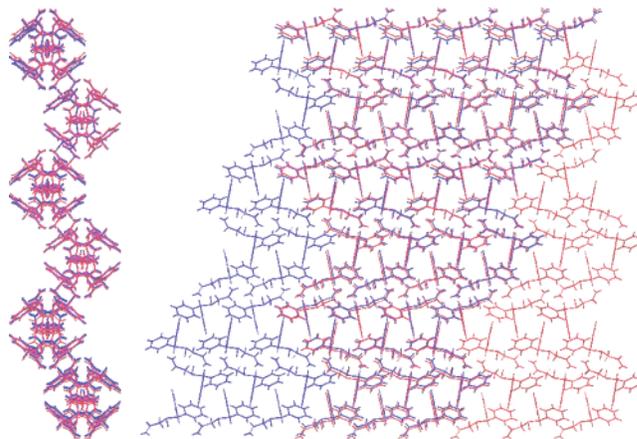**Figure 14.** (±) Modafinil form I ($P2_1/a$).

Figure 15. (±) Modafinil form III ($Pna2_1$) constructed by using the DCP model.

Figure 16. Superimposed structures of (±) modafinil form I (blue) and form III (red).

that the conformation differences between the two molecules (prime and nonprime) are ignored. Starting from the slice (002)B containing one molecule in the asymmetric unit (located in R1, R3, S2, and S4), one can add a 2-fold screw axis appropriately located and orthogonal to the PF to generate a daughter phase $Pna2_1$. In this new 3D packing, the inversion center and the internal 2-fold screw axis of the PF are not expressed anymore and thus become pseudo-symmetries. The number of independent molecules increases to $Z' = 2$. The daughter phase generated is identical to that constructed with the slice (002)A, conformations of the molecules 3 and 4 excepted.

To further study structural similarities and differences, the stacking of the common slice (002)A in both forms is investigated. Figure 14 and Figure 15 show the projection of the unit-cell of respectively form I and form
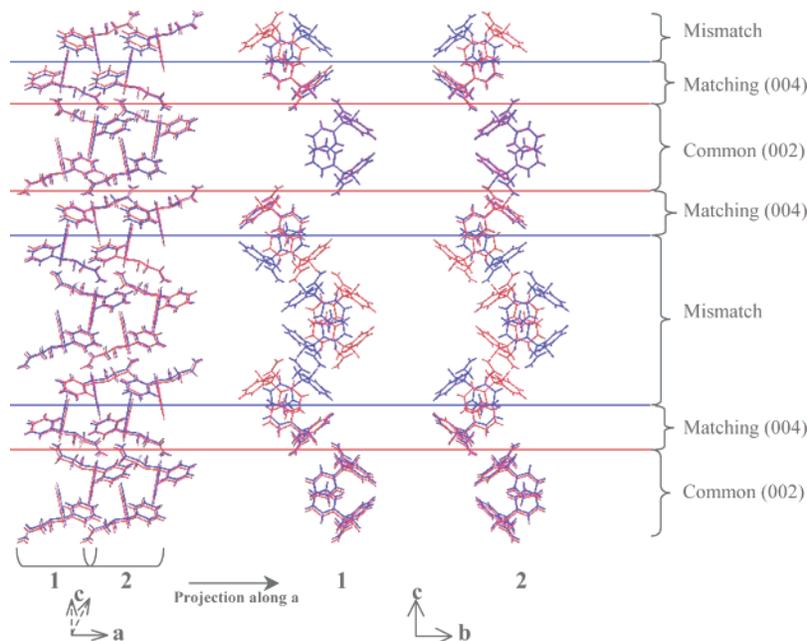
Figure 17. The observed (011) slice on the left is split into two slices and projected along *a* to allow the nonsuperimposable molecules to be seen. Form I is in blue and Form III is in red.
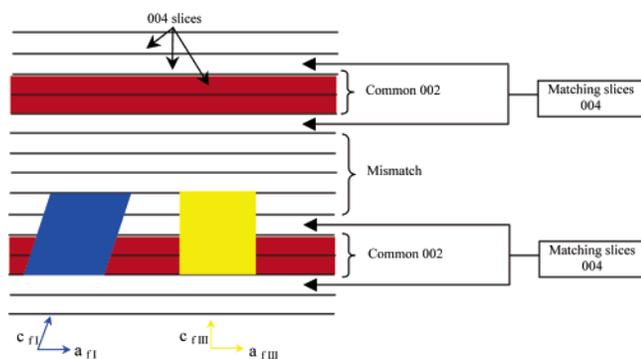

Figure 18. Stacking of (004) layers. Unit-cells of form I and III are respectively represented in blue and yellow.

III along *a* and *b*. These projections are then superimposed in Figure 16.

It can be observed that the packing seems at a first sight almost identical. Molecules matching between both structures are colored as depicted in Figure 17: the structures are split into two parts along the *a* parameter (see numbers 1 and 2 at the bottom of Figure 17).

As shown in Figure 17 and schematized in Figure 18, some (004) slices different from those contained in the common (002) slices are unexpectedly found to match between the orthorhombic and monoclinic structures. Even if these slices are generated from the common (002) slice, the molecules and the symmetry operators involved are different. The two 3D structures can be seen to be identical, with inclusion of defective slices of a height of a unit-cell leading either to form I or to form III.

Such a large structural analogy could easily lead to local defects in the crystals that would be difficult to detect. The packing could easily change from form I to form III along few (001) slices without significant alteration of the lattice energies.

Conclusion

The derived crystal packing model is a way to "predict" crystal structures having in common at least a monodimensional periodic fragment (PF). Starting from a known crystal structure, it consists of extracting a PF from the mother phase and in adding symmetry operators to regenerate a three-dimensional structure, i.e., daughter phase. Even if the conditions of a common PF appear to drastically reduce the applicability of the DCP model, several dozens of examples of pairs of polymorphs have been tested to work with this procedure[10] and many more are supposed to exist especially in the domain of metastable phases. In addition, the DCP model is of interest in the study of twins (and also lamellar epitaxies[26] of enantiomers) as it allows the prediction of possible structural arrangements at their interfaces. Aminov & Broomé[27] have long ago recognized that the structure at the interface is that of a possible polymorph.

In this paper starting from the original crystal structure of (±) modafinil form I, the DCP model is successfully applied to solve another crystal structure of (±) modafinil, namely, form III. Obviously, extensive structural relationships are found between both polymorphic forms. This results in a small difference between the energies of the two varieties, which is consistent with the observed concomitant polymorphism. It is also consistent with the slow kinetic of conversion of form III into form I in solution. In addition, the similarities could lead to the twinning of form I (however not yet observed). Further work will also be devoted to the explanation of the cross-shaped twins of form III.

The DCP model could be used as a routine method after a resolution of any crystal structure to detect possible polymorphic forms provided auxiliary information relevant to this model is available, such as common peaks at low θ on XRPD patterns, family of compounds

with a tendency to adopt the same packing, and heteronucleation of one form onto the other or twinning.

Supporting Information Available: Fractional coordinates, intramolecular distances, angles, torsion angles and hydrogen-bond distances for the daughter phase, the mother phase, and the minimized mother phase. This material is available free of charge via the Internet at http://pubs.acs.org.

References

(1) Bernstein, J.; Davey, R. J.; Henck, J.-O. *Angew. Chem., Int. Ed.* **1999**, *38*, 3440−3461.

(2) Burger, A.; Lettenbichler, A. *Pharmazie* **1993**, *48*, 262.

(3) Motherwell, W. D. S.; Ammon, H. L.; Dunitz, J. D.; Dzyabchenko, A.; Erk, P.; Gavezzotti, A.; Hofmann, D. W. M.; Leusen, F. J. J.; Lommerse, J. P. M.; Mooij, W. T. M.; Price, S. L.; Scheraga, H.; Schweizer, B.; Schmidt, M. U.; van Eijck, B. P.; Verwer, P.; D. E. Williams *Acta Crystallogr. B* **2002**, *58*, 647−661.

(4) Perlstein, J. *J. Am. Chem. Soc.* **1994**, *116*, 11420−11432.

(5) Gavezzotti, A. PROMET 5.3. A Program for the Generation of Possible Crystal Structures from the Molecular Structure of Organic Compounds. University of Milan, Italy, 1997.

(6) Kitaigorodskii, A. I. *Organic Chemical Crystallography*; Consultants Bureau; New York, 1961; pp 65−112.

(7) Dunitz, J. D. *Chem. Commun.* **2003**, 545−548.

(8) Desiraju, G. R. *Angew. Chem. Ed. Engl.* **1995**, *34*, 2311−2327.

(9) Sarma, J. A. R. P.; Desiraju, G. R. *Cryst. Growth Des.* **2002**, *2*, 93−100.

(10) Gervais, C.; Coquerel, G. *Acta Crystallogr. B* **2002**, *58*, 662−672.

(11) Orsymonde US Patent 60402064.

(12) Teva US Patent 4177693 and US Patent 5180745.

(13) Grimbergen, R. F. P.; Meekes, H.; Bennema, P.; Strom, C. S.; Vogels, L. J. P. *Acta Crystallogr*. **1998**, *A54*, 491−500.

(14) Gavezzotti, A.; Filippini, G. *J. Am. Chem. Soc.* **1995**, *117*, 12299−12305.

(15) Cerius², Accelrys Inc., version 4.6, Cambridge, U.K., website: www.accelrys.com.

(16) SYBYL 6.8, Tripos Associates: St Louis, MO, website: www.tripos.com.

(17) Clark, M.; Cramer, R. D.; Van Opdenbosch, N. *J. Comput. Chem.* **1989**, *10*, 982−1012.

(18) Goodford, P. J. *J. Med. Chem.* **1985**, *28*, 849−857.

(19) Mayo, S. L.; Olafson, B. D.; Goddard, W. A. *J. Phys. Chem.* **1990**, *94*, 4, 8897−8909.

(20) Stewart, J. J. P. *J. Comput.-Aided Mol. Des.* **1990**, *4*, 1−105.

(21) Dewar, M. J. S.; Zoebish, E. G.; Healy E. F.; Stewart, J. J. P. *J. Am. Chem. Soc.* **1985**, *107*, 3902−3909.

(22) Zorky, P. M. *J. Mol. Struct.* **1996**, *374*, 9−28.

(23) Petit, S.; Coquerel, G.; Hartman, P. *J. Cryst. Growth* **1994**, *137*, 585−594.

(24) Kuleshova, L. N.; Antipin, M. Yu. *Kristallografiya* **2002**, *48*, 293−314.

(25) Courvoisier, L.; Mignot, L.; Petit, M. N.; Coquerel, G. *Org. Proc. Res. Dev.* **2003**, *7*, 1007−1016.

(26) Gervais, C.; Beilles, S.; Cardinaël P.; Petit S.; Coquerel, G. *J. Phys. Chem. B* **2002**, *106*, 646−652.

(27) Aminoff, G.; Broomé, A. *Z. Krist.* **1931**, *80*, 355.

CG030069T